GSC Biological and Pharmaceutical Sciences, 2020, 12(01), 102-115

Available online at GSC Online Press Directory

GSC Biological and Pharmaceutical Sciences

e-ISSN: 2581-3250, CODEN (USA): GBPSC2

Journal homepage: https://www.gsconlinepress.com/journals/gscbps

(RESEARCH ARTICLE)

# Toxicity evaluation of $TiO_2$ nanoparticles embedded in toothpaste products

Al-Salman Fadheela [1], Ali Redha Ali [1,*], Al-Shaikh Hawraa [1], Hazeem Layla [2] and Taha Safa [3]

[1] *Department of Chemistry, College of Science, University of Bahrain, Sakhir, Kingdom of Bahrain.*
[2] *Department of Biology, College of Science, University of Bahrain, Sakhir, Kingdom of Bahrain.*
[3] *Princess Al-Jawhara Bint Ibrahim Al-Ibrahim Centre for Molecular Medicine, Genetics and Inherited Diseases, Manama, Kingdom of Bahrain.*

Publication history**:** Received on 27 June 2020; revised on 06 July 2020; accepted on 09 July 2020

Article DOI: https://doi.org/10.30574/gscbps.2020.12.1.0205

## Abstract

The present study evaluates the toxicity of titanium dioxide nanoparticles ($TiO_2$ NPs) that were extracted from toothpaste products by solid-liquid extraction method. The NPs structures were characterized using X-ray diffraction (XRD), Fourier-transform infrared spectroscopy (FTIR) and scanning electron microscope (SEM). Ultraviolet spectrophotometer (UV) was also used to determine the band gab energy of these NPs. The XRD results indicated that the mixture of $TiO_2$ NPs was formed (anatase and rutile titanium dioxide nanoparticles). XRD results also indicated the crystalline size of NPs, which were small and ranging from 2.5 to 53.2 nm. The toxicity effect of $TiO_2$ NPs was evaluated on *Chlorella vulgaris* micro marine algae over 3 days. The results indicate a negative effect on the growth algae and concentration of chlorophyll a during the early growth stages. In contrast, at the late growth stages these NPs had a positive effect. Also, the toxicity effect of $TiO_2$ NPs was evaluated on Jurkat, HepG2, T-47D and S180 cancer cell lines. Cells were cultured with various concentrations of $TiO_2$ NPs (10, 20, 50, 100 and 200 µg/mL) for 48 hours using the Water-Soluble Tetrazolium (WST) method. The results showed that the $TiO_2$ NPs had a negative effect on the growth of the Jurkat, T-47D and S180 cancer cell lines. In contrary, a positive effect was seen on the HepG2 cell line.

**Keywords:** Titanium dioxide nanoparticles; Biotoxicity; Jurkat; HepG2; T-47D; S180.

## 1. Introduction

### 1.1. Titanium dioxide nanoparticles

Titanium dioxide nanoparticles (commonly referred to as nano-$TiO_2$ or $TiO_2$ NPs) belong to the transition metal oxides family. In nature, there are three commonly known polymorphs of titanium dioxide nanoparticles: rutile (tetragonal), anatase (tetragonal), and brookite (orthorhombic) [1]. In addition to these polymorphs, two high pressure forms have been synthesized from rutile phase: (a) $TiO_2$ (II) with a $PbO_2$ structure, and (b) $TiO_2$ (H) with a hollandite structure [2].

In recent years, $TiO^2$ NPs have been used in a wide range of industrial applications, due to their unique advantages such as brightness, having very high refractive index, low cost, being highly stable, anticorrosive, and being non-toxic to humans [3], [4]. In addition, these unique properties make $TiO_2$ NPs ideal to be used in various personal care products (PCPs) such as cosmetics, sunscreens, toothpastes, and skin care products. Currently, many PCPs containing $TiO_2$ NPs are investigated as novel treatments for acne vulgaris, hyperpigmented skin lesions, atopic dermatitis, and other non-dermatologic diseases [5]. $TiO_2$ NPs have also shown antibacterial activity against some pathogenic bacteria [6]. In the field of nanomedicine, $TiO_2$ NPs are useful tools in advanced imaging and nanotherapeutics, for example, in photodynamic therapy (PDT) [4]. $TiO_2$ NPs have been evaluated as potential photosensitizers [7]. Also, $TiO_2$ NPs are used as drug for cancer cell treatment [8].

* Corresponding author: Ali Redha Ali, Emal: ali96chem@gmail.com

### 1.2. Biotoxicity of $TiO_2$ NPs

As $TiO_2$ NPs are used in many fields such as industry and agriculture, they can easily be released in the environment. As a result of the spread of these nanoparticles in the environment, it may affect marine organisms such as algae which forms the base of many food-webs, and also contribute to the self-purification of polluted water [9], [10]. Algae may be sensitive to $TiO_2$ NPs and can impact other types of organisms like fish and invertebrates [9], [10].

The ecotoxicity of $TiO_2$ NPs to algae have been described in some studies, where $TiO_2$ NPs decreased algal growth and total chlorophyll content [11], [12]. In contrast, $TiO_2$ NPs were found to have no effect on activity of some algae after short term exposure at concentrations up to 100 mg/L and may even stimulate growth rates at low concentrations (0-10 mg/L), facilitate electron transport in plants and stimulate photosynthesis [13], [14]. Furthermore, certain types of algae have been engineered to incorporate $TiO_2$ into their tissues to enhance photo-efficiency [15]. Some studies demonstrated the ecotoxicity of cadmium to algae in the presence and absence of $TiO_2$ with a concentration of 2 mg/L, and the presence of $TiO_2$ in algal tests reduced the observed toxicity due to a decrease in bioavailability of cadmium resulting from sorption, and complexation of $Cd^{2+}$ ions onto the $TiO_2$ surface [13]. Given these contrasting results of $TiO_2$ NPs, the toxicity mechanisms of $TiO_2$ NPs to microalgae are still unknown.

In this study, the cumulative effect of $TiO_2$ NPs of a specific concentration has been evaluated on microalgae. Batch cultured Chlorella vulgaris were employed as testing organism to investigate their growth, morphological changes, and their chlorophyll a content under NPs exposure.

### 1.3. Anti-cancer activity of $TiO_2$ NPs

Nowadays, cancer is the second most common diseases cause of death in the world. Treatment of patients with cancer remains a challenge due to the disappointing effects of most conventional treatments like chemotherapies and radiotherapies. The most common drawback of all conventional treatments is that they are very imprecise due to a lack of selectivity between malignant and healthy cells [13]. In contrast, nanotechnology offers a vision for a new approach to fight cancer tumors due to the ability of nanoparticles to locate cancer cells and destroy them with single-cell precision which is due to their unique physicochemical properties [16]. One type of these nanoparticles is $TiO_2$ NPs which can drive various chemical reactions due to their strong oxidizing and reducing ability, $TiO_2$ NPs can also affect cellular functions [8]. Depending on these properties, $TiO_2$ NPs are considered one of the most common nanoparticles used in cancer cell treatment [8]. Thevenot et al. examined the anticancer effect of $TiO_2$ NPs on several types of cancer and control cell lines. They confirmed that the cell viability depends on particles concentration [17]. Also, they suggested that $TiO_2$ NPs can be surface engineered for targeted cancer therapy [17].

In this research, the effect of various concentrations of $TiO_2$ NPs on the growth inhibition of four cell lines (Jurkat, HepG2, T-47D, and S180) has been examined by water soluble tetrazolium (WST) assay. WST is one of the assays that can measure the metabolic activity, and is suitable to measure cell proliferation, cell viability, and cytotoxicity in mammalian cells. The WST protocol is based on the cleavage of the tetrazolium salt WST to form colored formazan by cellular mitochondrial dehydrogenases. If the number of viable cells is large and the activity of the mitochondrial dehydrogenases is high, the amount of formazan dye increases [18].

## 2. Material and methods

### 2.1. Sample extraction

#### *2.1.1. Materials*

Four types of commercial toothpaste, n-hexane ($C_6H_{14}$), and absolute ethanol ($C_2H_5OH$).

#### *2.1.2. Extraction of $TiO_2$ from toothpaste products*

Titanium dioxide nanoparticles were extracted from toothpastes following the modified version of the protocol developed by Barker et al. [19]. About 3.0 g of each type of toothpaste was weighed in a 40 mL centrifuge tube using precision scale and mixed with 30 ml of n-hexane. The mixture was shaken for 1 min, and centrifuged (4000 rpm, 5 min) using CS-6 centrifuge. Subsequently, the hexane solvent with the suspended materials was decanted, and 30 mL of absolute ethanol was added to the residue left at the bottom of the tube. The mixture was shaken for 1 min, and centrifuged (4000 rpm, 5 min). The ethanol solvent with the suspended materials was decanted from the tube. After that, 30 mL of distilled water was added to the tube, the mixture was then shaken for 2 min, and centrifuged (3000 rpm, 10 min), and the supernatant was decanted (repeated two times). Thereafter, the residue left at the bottom of the tube

was transferred into a 15 mL crucible and placed in oven 2 h at 700 °C, then the crucible was kept in a desiccator. At the end, enough titanium dioxide nanoparticles (in the form of nano-powder) was obtained. To further refine, the obtained nano-powders were grinded using sterilized manual grinder. The procedure was done three times for each product.

### 2.2. Characterization of $TiO_2$ nanoparticles

#### *2.2.1. X-ray diffraction (XRD)*

Extracted samples were analyzed using Philips diffractometer that was equipped with Cu Kα radiation (λ = 1.542 Å), and acceleration voltage of 40 kV. The data were recorded with a counting rate of 1°/min.

#### *2.2.2. Scanning electron microscopy (SEM)*

The morphological observations for the prepared samples was performed using ZEISS EVO LS 10 scanning electron microscope (SEM) with acceleration voltage of 20 kV.

#### *2.2.3. Fourier transform infrared spectroscopy (FTIR) analysis*

SHIMADZU FTIR spectrophotometer, and WinFirst spectroscopy software were used to determine the various functional groups present in $TiO_2$ NPs. FTIR spectra of the prepared nanoparticles were collected by pressing the particle sample with KBr powder to form pellets.

#### *2.2.4. Ultraviolet spectrophotometer (UV) analysis*

The absorbance of $TiO_2$ NPs was measured by Lambda XLS spectrophotometer to determine the band gap energy $E_g$. A solution of $1 \times 10^{-2}$ M of $TiO_2$ NPs was prepared by dissolving 0.008 g of nanoparticles in 10 mL of distilled water.

### 2.3. Biotoxicity assay

#### *2.3.1. Materials*

Muse Count and Viability Assay Kit, magnesium chloride ($MgCl_2$), and 90 % acetone HPLC grade.

#### *2.3.2. Chlorella vulgaris culture*

A pure culture of *Chlorella vulgaris* was obtained from National Marine Culture Centre, Ministry of Municipalities and Urban Planning, Kingdom of Bahrain.

In each one of three 2 L Erlenmeyer flasks, microalga was grown in 1 L of sterilized medium that was prepared with filtered seawater. After that, the Erlenmeyer flasks were capped with loose cotton and placed in an illuminated incubator with continuous illumination of approximately 100 μmol $m^{-2}$ $s^{-1}$ at 18 °C. The Walne's medium was used and 8 value was the initial pH value. The cell density of the culture was monitored microscopically every 24 h and the different growth phases were determined by counting with a hemocytometer and Olymous CX21 microscope. Morphological observations were conducted with a Zeiss HB100 microscope.

#### *2.3.3. Algal growth assays*

All cultures were incubated with $TiO_2$ NPs at the lag phase. Viable cell counts and the measurements of chlorophyll a concentration were performed starting from the second day to fourth day of inoculation. Three replicates for each test culture in addition to the control were prepared. Assay was run with $TiO_2$ (10 mg/L), where 1.5 mg of $TiO_2$ NPs were dissolved in 150 mL of the culture into 250 mL Erlenmeyer flask. A concentration of 10 mg/L of $TiO_2$ NPs was chosen based on the findings of Ji et al. [20]. Also, three replicates of control were prepared, where 150 mL of culture was placed in the Erlenmeyer flask without $TiO_2$ NPs. Subsequently, all cultures (control and treated algae) were incubated in an illuminated incubator with continuous high shaking speed (150 r/min) to reduce aggregation and settlement of the NPs over the incubation period. Changes in viable cell concentration were measured using MuseTM Cell analyzer, where 50 μL of the prepared sample was placed in the microcentrifuge tube, and 450 μL of the Muse Count and Viability Assay was added. The Muse Count and Viability Assay Kit provided rapid and reliable determinations of viability and total cell count using the MuseTM Cell Analyzer. The Muse™ Cell Analyzer uses miniaturized fluorescent detection and microcapillary technology to deliver quantitative cell analysis of both suspension and adherent cells from 2 to 60 μm in diameter.

Additionally, chlorophyll a concentration was determined, where 30 mL of each algal culture was filtered, and a spatula of $MgCl_2$ was added to the residue in the filter paper. Filter paper, residue, and $MgCl_2$ were dissolved in 10 mL of 90 %

acetone by manual grinder, and the mixture solution was poured in 15 mL glass centrifuge tube. After that, the solution was centrifuged (4000 rpm, 10 min) using CS-6 centrifuge to extract chlorophyll a. Subsequently, the solution that contained chlorophyll a was diluted with 90 % acetone to prepare a 25 mL solution. Then, the absorbance of chlorophyll a was measured at 630, 645, 663, and 750 nm using Lambda XLS spectrophotometer to determine the concentration. The procedure was repeated three times for each type of extracted $TiO_2$ NPs.

### 2.4. Toxicity of $TiO_2$ NPs on cell lines

#### *2.4.1. Materials*

10 % Fetal bovine serum (FBS), 0.25 % (w/v) trypsin- 0.53 mM EDTA solution, 0.2 units/mL bovine insulin, and water-soluble tetrazolium solution.

#### *2.4.2. Cell line culture*

Four cell lines, including three human cell lines: Jurkat cell line, HepG2 human liver cancer cell line, and T-47D human breast cancer cell line, and S180 murine Sarcoma cancer cell line were used in this study. All cultures were prepared and placed in 96 well culture plate, where each type of cell culture occupied three columns with $10^4$ cell/well without the first row of the plate, which contained appropriate culture media as a blank. Final volume of culture medium in each well was 100 µL. Culture plate was incubated for 24 h in cell culture incubator at 37 °C, with 5 % $CO_2$ in air atmosphere.

Jurkat culture: Base medium for Jurkat cell line was ATCC-formulated RPM 1640 Medium, Catalog No. 30 2001. The growth medium was completed by added 10 % FBS to the base medium. To prepare the culture, culture flask was seeded with cells, grown, and filled with base medium to prevent loss of cells during shipping. Subsequently, the flask was incubated in an upright position for several hours at 37 °C. After equilibration of temperature, the entire contents of the flask were removed and centrifuged (4000 rpm, 5 to 10 minutes) using ROTINA 380 R. Then, the medium was removed and saved for reuse, and cell pellet was resuspended in 10 mL of this medium. Finally, the culture was incubated in cell culture incubator horizontally at 37 °C with 5 % $CO_2$ in air atmosphere.

HepG2 culture: Base medium for HepG2 cell line was ATTCC-formulated Eagle's Minimum Essential Medium, Catalog No. 30 2003. The growth medium was completed by added 10 % FBS to the base medium. At the beginning, the cells were gown in the culture media in the cell culture dish. After that, the culture media was removed, and the cell layer was briefly rinsed with Trypsin-EDTA solution to remove all traces of serum that contain trypsin inhibitor. Subsequently, 2.0 to 3.0 mL of Trypsin-EDTA solution were added to the dish, and cells were observed under an inverted microscope until cell layer was dispersed (within 5 to 15 min). Then, 6.0 to 8.0 mL of complete growth medium and aspirate cells were added by gently pipetting. Appropriate aliquots of the cell suspension were added to new culture dishes. Finally, cultures were incubated in cell culture incubator at 37 °C with 5 % $CO_2$ in air atmosphere.

T-47D culture: Base medium for T-47D cell line was ATCC-formulated RPMI-1640 Medium, Catalog No. 30 2001. The growth medium was completed by added 10 % FBS, and 0.2 units/mL bovine insulin to the base medium. Culture was prepared by the same procedure which was followed to prepare HepG2 culture.

S180 culture: Base medium for S180 cell line was ATCC-formulated Dulbecco's Modified Eagle's Medium, Catalog No. 30 2002. The growth medium was completed by adding 10 % of FBS to the base medium. Culture was prepared by the same procedure which was followed to prepare Jurkat culture.

#### *2.4.3. Cell Growth Assays*

After one day of incubation of the cell culture plate, cells were incubated with different concentrations of $TiO_2$ NPs solution for a defined time (48 hours). A solution of 200 µg/mL of $TiO_2$ NPs was prepared by dissolved 20 mg of $TiO_2$ NPs (extracted from toothpaste sample D) in 10 mL distilled water and sonicated for 1 min using Soniprep 150 plus. After that, 100, 50, 20, and 10 µg/mL of $TiO_2$ NPs solutions were prepared by serial dilution. In the first row of cell culture plate, only appropriate culture media as blank was placed in the wells. The second row of the culture plate was considered as positive control (PC), where 0.4 µM of cytotoxic staurosporine was added to the cell culture in the wells. While the third row was considered as negative control (NC), where the cell culture remained alone without any addition. In the remaining rows, the cell cultures were treated by 10 µL of 10, 20, 50, 100, and 200 µg/mL of $TiO_2$ NPs solutions, respectively.

## 3. Results and discussion

### 3.1. Sample extraction

In this research $TiO_2$ NPs were extracted from four types of toothpaste products, Table 1 summarizes the compositional characteristics of the four toothpastes.

**Table 1** Identification and composition of toothpastes employed in the study**.**

| Toothpaste type | Inorganic compounds | Organic compounds |
|---|---|---|
| A | $TiO_2$, NaF, and hydrated silica. | $C_6H_{14}O_6$, $C_5H_{12}O_5$, $C_2H_6O_2$, $CH_3(CH_2)_{11}SO_4Na$, $C_8H_8O_3$, $C_{11}H_{14}O_3$ |
| B | $TiO_2$, NaOH, $KNO_3$, NaF, hydrated silica, and $Na_5P_3O_{10}$. | $C_6H_{14}O_6$, $C_3H_8O_3$, $C_{10}H_{16}$, $C_{35}H_{49}O_{29}$, $C_7H_5NO_3S$, and CAPB. |
| C | $TiO_2$, NaOH, $KNO_3$, NaF, and hydrated silica. | $C_6H_{14}O_6$, $C_3H_8O_3$, $C_{12}H_{19}Cl_3O_8$, $C_{35}H_{49}O_{29}$, $C_7H_5NO_3S$, and CAPB. |
| D | $TiO_2$, $NaHCO_3$, NaF, and hydrated silica. | $C_3H_8O_3$, $C_{35}H_{49}O_{29}$, $C_7H_5NO_3S$, and CAPB. |

To separate the active organic and inorganic compounds in the toothpaste solid-liquid extraction was implemented. In this study, the first solvent used for extraction was n-hexane, after shaking and centrifuging, hexane extracted the active organic compounds which was then decanted to give a clear organic phase. The second extracting solvent was absolute ethanol, it was used to extract the remaining organic compounds leaving the inorganic compounds and surfactants. The last solvent was distilled water which was used to extract the polar water-soluble inorganic compounds and surfactants. The residue containing insoluble inorganic compounds ($TiO_2$ NPs) was dried in laboratory oven for 2 h at 700 °C to remove any remaining of solvents. Then, to protect the compounds from humidity, the dried residue was kept in a desiccator. At the end, enough titanium dioxide nanoparticles (in the form of nano-powder) was obtained. For further refining, the obtained nano-powders were grinded in a sterilized manual grinder. The extracted inorganic compounds were characterized by XRD, SEM, FTIR, and UV spectrophotometer.

### 3.2. XRD analysis

XRD analysis was used to identify the crystalline phase composition and the crystallites size of the extracted $TiO_2$ NPs. The results were plotted as peak positions at 2θ and X-ray counts (intensity) in the form of an x-y plot.

The crystallite size of all extracted samples has been calculated by Debye-Scherer formula [$D = 0.94\lambda/ (\beta \cos \theta)$], where D is the crystallite size, λ is the X-ray wavelength (1.542 Å for Cu-Kα radiation), β is the full width half maxima (FWHM) of the diffraction peaks, and θ is the Bragg's angle.

Table 2 Summarizes XRD analysis data in terms of crystalline phase composition and crystalline size. The XRD patterns of the extracted samples are shown in Figures 1, 2, 3 and 4.

**Table 2** XRD analysis data (crystalline phase composition and crystal size) of crystal sample.

| Sample | Crystalline phase composition | Crystallite size (nm) |
|---|---|---|
| A | Anatase | 53.2 |
| B | Rutile | 2.5 |
| C | Anatase | 35.5 |
| D | Rutile | 36.4 |

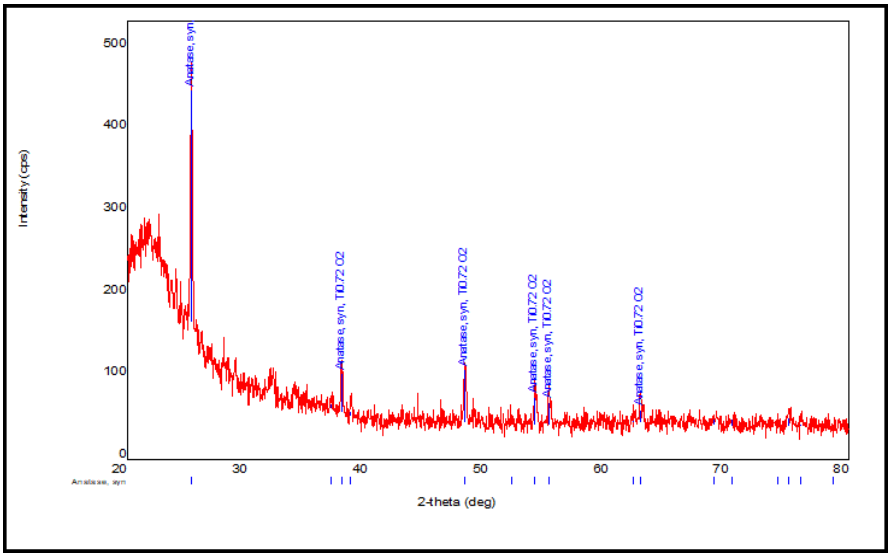


**Figure 1** XRD patterns of the single anatase $TiO_2$ NPs from sample A.

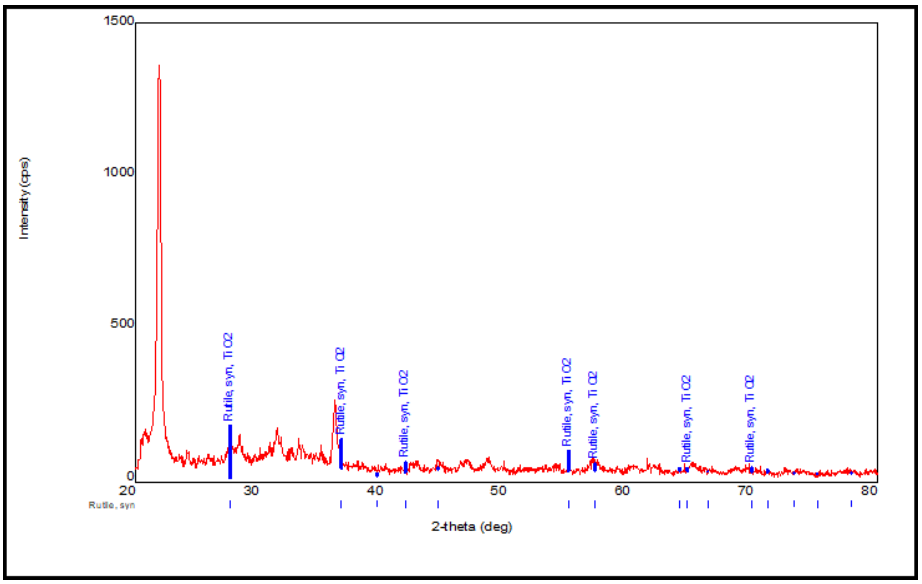


**Figure 2** XRD patterns of the single rutile $TiO_2$ NPs from sample B.

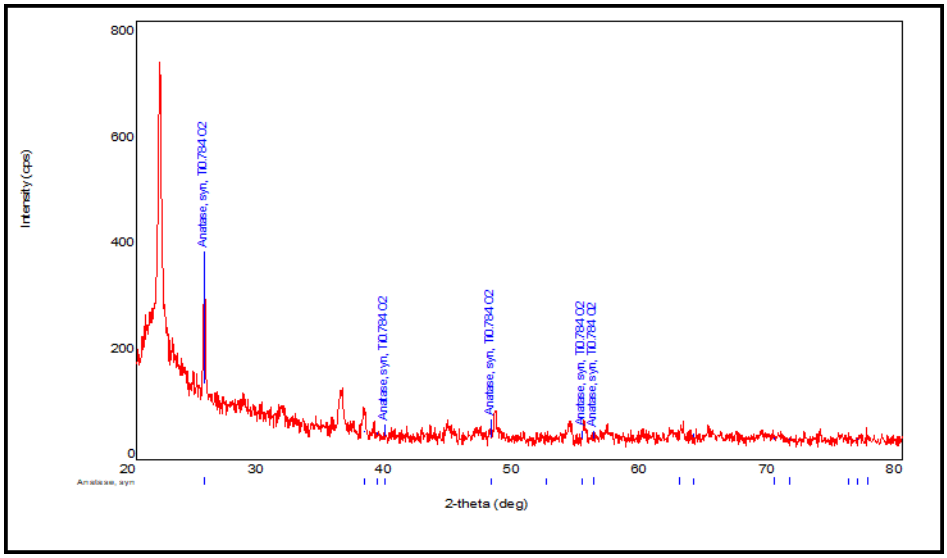


**Figure 3** XRD patterns of the single anatase $TiO_2$ NPs from sample C.

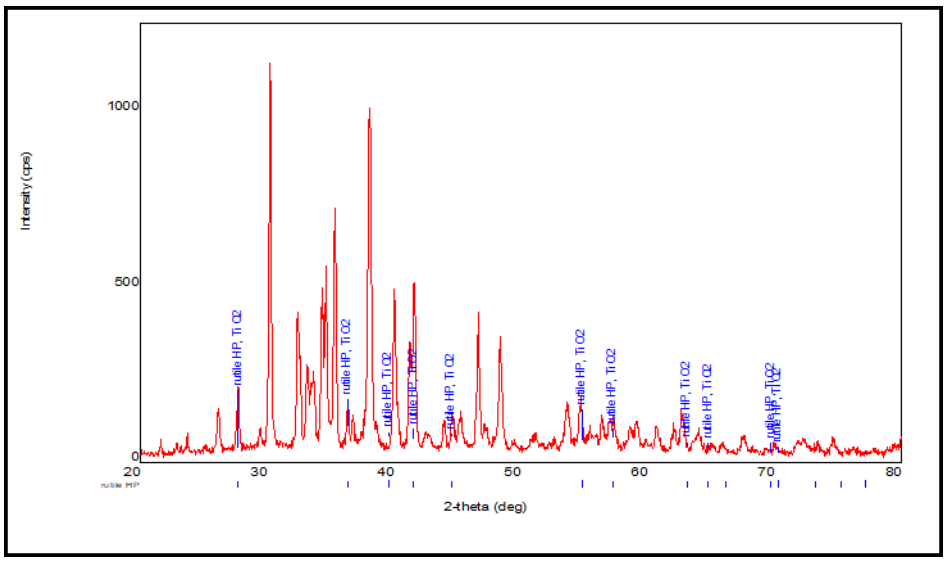


**Figure 4** XRD patterns of the single rutile TiO2 NPs from sample D.

The XRD results agree with the reported XRD pattern of anatase and rutile $TiO_2$ NPs. A single anatase phase of the $TiO_2$ from sample A and C was identified, while a single rutile phase from sample B and D was identified. Since the crystallite size of all samples are less than 100 nm, all samples were considered as nanoparticles.

### 3.3. SEM analysis

The surface morphology of the extracted samples was characterized by SEM. The SEM images of $TiO_2$ NPs are shown in Figure 5.

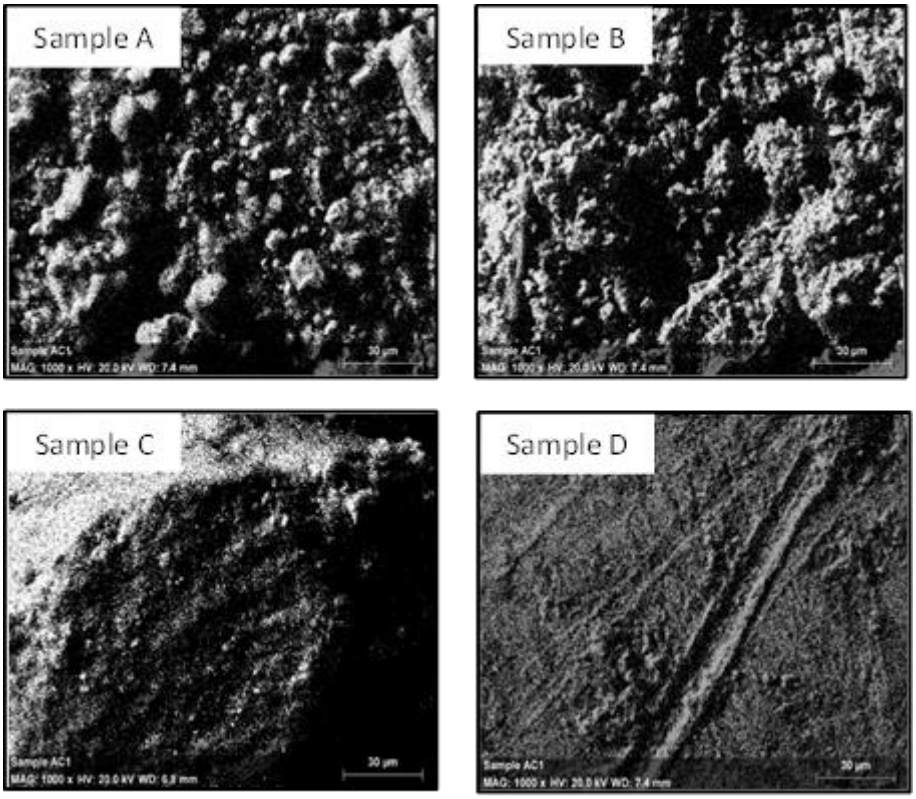


**Figure 5** SEM images of $TiO_2$ NPs extracted from each toothpaste sample

### 3.4. FTIR analysis

FTIR analysis was performed on extracted $TiO_2$ NPs to identify the composition and functional groups present in the samples. FTIR spectra was obtained for all samples, at a range of 250-4000 $cm^{-1}$ at room temperature. FTIR spectra of $TiO_2$ NPs included bands at 3200-3600 $cm^{-1}$, and 1630-1800 $cm^{-1}$ due the stretching vibration and bending vibration of OH, respectively. In the spectrum of synthesized $TiO_2$ NPs, the peaks at 500-900 $cm^{-1}$ showed stretching vibration of Ti-O-Ti and stretching vibration of Ti-O [21]. Table 3 shows the bands wavelength in $cm^{-1}$ of all groups present in the samples which were within the range of reported values.

**Table 3** The bands wavelength in $cm^{-1}$ of all groups present in the samples.

| Sample | Vibrations ($cm^{-1}$) | | | |
|---|---|---|---|---|
| | OH-stretching | OH-bending | Ti-O-Ti stretching | Ti-O stretching |
| A | 3441.01 | 1643.35 | 802.39 | 473.35 |
| B | 3402.43 | 1651.07 | 786.96 | 486.06 |
| C | 3448.72 | 1635.64 | 786.96 | 478.35 |
| D | 3271.27 | 1774.51 | 694.37 | 501.49 |

### 3.5. UV analysis

The absorbance of all extracted samples was measured by Lambda XLS spectrophotometer to determine the band gap energy depending on the plank's equation ($E = h\nu$), where E is the band gap energy, h is the plank's constant ($h = 6.626 \times 10^{-34}$ J s) and $\nu = c / \lambda$, where c is the speed of light and $\lambda$ is the wavelength of the spectrum. Table 4 shows the absorbance wavelength (nm) and the absorbance of all samples.

**Table 4** The absorbance wavelength and the absorbance of all extracted samples.

| Sample | Wavelength (nm) | Absorbance (A) |
|---|---|---|
| A | 350 | 0.566 |
| B | 350 | 0.069 |
| C | 350 | 0.086 |
| D | 350 | 0.114 |

The band gap energy of extracted samples was calculated to be 3.5 eV which was close to the energy band gap value of $TiO_2$ NPs used in nanotechnology applications (equal to 3.2 eV).

### 3.6. Cumulative effect of $TiO_2$ NPs on algal growth

Nanoparticles have different physicochemical properties which can affect their interactions with different organisms, their size and/or surface area highly affects their interactions. The toxicological effects of NPs depends on their chemical composition, size, test method and test organisms [22]. When considering the interactions of NPs with algae, the type of NPs, the tendency to compete with another ionic nutrients for uptake, and dissolution are important factors to consider [12]. For instance, the toxicity effect of $TiO_2$ NPs on *Desodesmus subspicatus*, a green algae, has shown that it depends on the surface area of the NPs, where the smallest particles caused high toxicity while the larger ones have opposite effect [23]. Also, similar trend was observed by other scientists, larger $TiO_2$ NPs gave rise to small inhibition compared to the smaller NPs [13].

As shown in Figure 6, the growth curve of the control culture was normal, the concentration of viable cells during the exponential growth phase reached to the maximum ($3.96 \times 10^5$ viable cell/mL). In treated sample cultures A, B, C and D, the number of viable cells were lower number compared to the control culture during the first growth stage. On the other hand, during the decline phase the viable cell number was higher in the treated samples, while the control culture during the decline phase had a lower number of viable cells. Detailed results are shown in Table 5.

**Table 5** The effect of $TiO_2$ NPs on the growth of *Chlorella vulgaris*. The values are reported as mean of 3 replicates ± standard deviation.

| Sample | Cell Count (viable cell/mL) x $10^5$ | | |
|---|---|---|---|
| | 24 hours | 48 hours | 72 hours |
| Control | 3.053 ±0.367 | 3.960 ±0.030 | 3.933 ±0.482 |
| A | 3.027 ±0.423 | 2.967 ±0.321 | 4.083 ±0.126 |
| B | 2.953 ±0.649 | 2.713 ±0.506 | 4.317 ±0.076 |
| C | 2.863 ±0.197 | 2.643 ±0.276 | 4.467 ±0.153 |
| D | 2.997 ±0.260 | 2.77 ±0.142 | 4.243 ±0.051 |

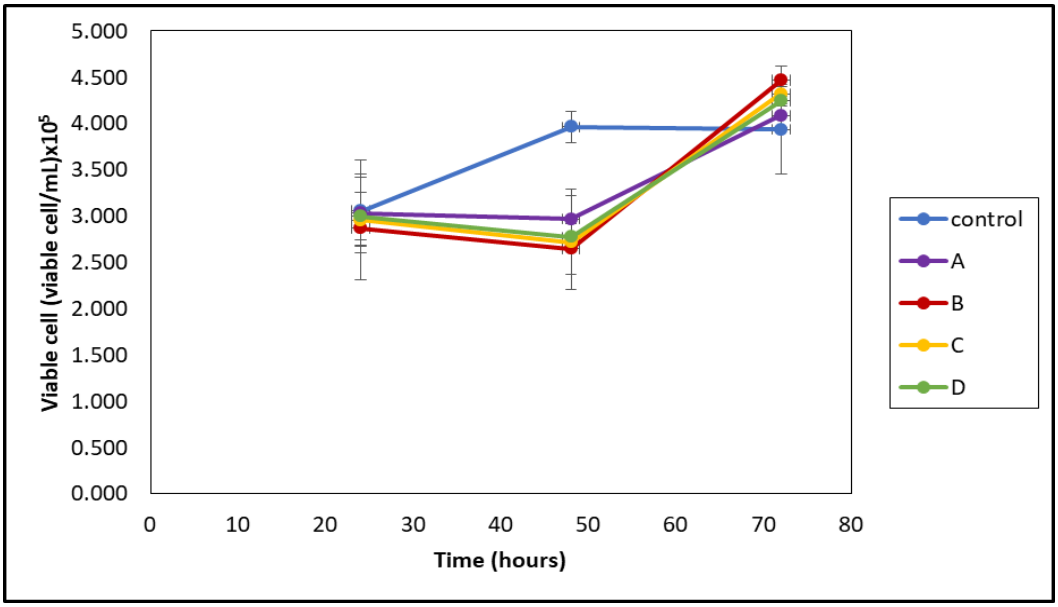


**Figure 6** The effect of $TiO_2$ NPs on the growth of *Chlorella vulgaris*. The values are reported as mean of 3 replicates ± standard deviation.

Figure 7 illustrates the effect of $TiO_2$ NPs on the concentration of chlorophyll a in *Chlorella vulgaris*. In general, the curves of chlorophyll a content showed similar pattern as the curves of growth cells. During the exponential growth phase, the highest chlorophyll a concentration in the control culture was achieved, 1.225 µg/mL, and this concentration was corresponding to the viable cells' concentration. In contrast, the treated cultures contained a lower concentration of chlorophyll a, as the cell count in the first growth stage. During the decline phase, the highest chlorophyll a concentration was present in treated sample cultures while the lowest chlorophyll a concentration was in the control culture. Detailed results are shown in Table 6.

**Table 6** The effect of $TiO_2$ NPs on Chlorophyll a content of Chlorella vulgaris. The values are reported as mean of 3 replicates ± standard deviation.

| **Sample** | **Chlorophyll a Concentration (µg/mL)** | | |
|---|---|---|---|
| | 24 hours | 48 hours | 72 hours |
| **Control** | 1.022 ±0.145 | 1.225 ±0.090 | 1.084 ±0.201 |
| **A** | 1.011 ±0.106 | 0.933 ±0.314 | 2.315 ±0.297 |
| **B** | 1.024 ±0.249 | 0.659 ±0.066 | 3.178 ±0.050 |
| **C** | 1.036 ±0.209 | 0.747 ±0.082 | 2.876 ±0.421 |
| **D** | 1.096 ±0.075 | 0.821 ±0.040 | 2.678 ±0.141 |

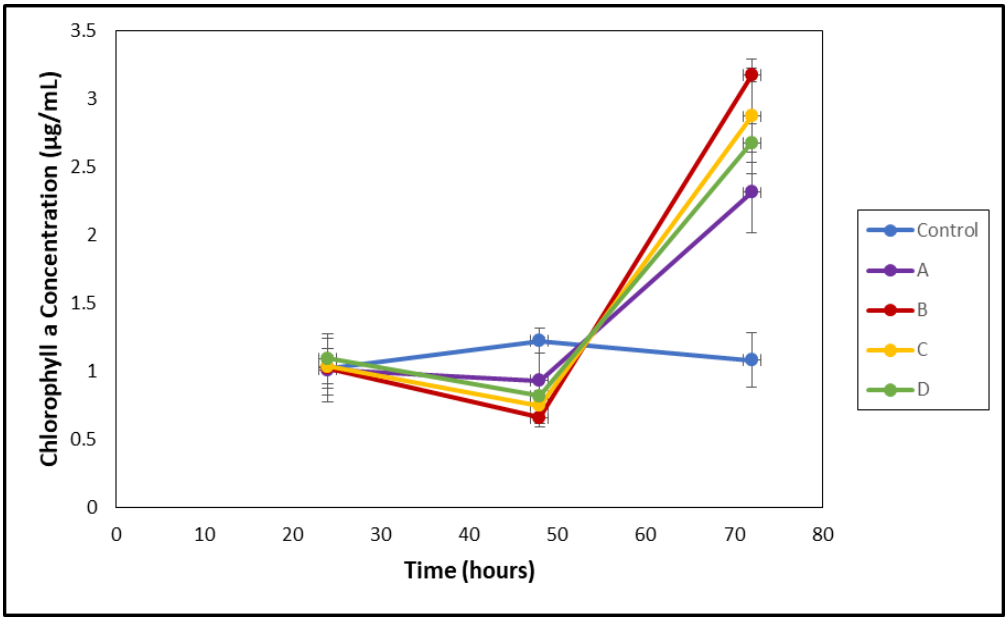


**Figure 7** The effect of $TiO_2$ NPs on Chlorophyll a content of *Chlorella vulgaris*. The values are reported as mean of 3 replicates ± standard deviation.

The results showed that $TiO_2$ NPs had a negative effect on the growth algae and concentration of chlorophyll a during the early growth stages. In contrast, at late growth stages, these NPs had a positive effect. Also, the effect of NPs was dependent on their size, where the smallest sample of NPs (sample B) of a size of 2.5 nm exhibited dramatic effect on the algae growth and chlorophyll a concentration. Samples C and D had approximately same size 35.5 nm and 36.4 nm respectively, showed less effect compared to the sample B. While the largest, sample A, with a size of 53.2 nm displayed the least effect.

### 3.7. Cumulative effect of $TiO_2$ NPs on cancer cell lines

As mentioned earlier, nanoparticles have different properties which can affect their interactions with organisms. The steric stabilization property is considered as the most important properties of NPs which led to increasing the stability of NPs in the biological systems, this property provides the opportunity to use the NPs in drug delivery systems (DDS) [24]. The major reason for using NPs in DDS is the ability to control the characteristics and the size of NPs. Due to these properties NPs are used in many medical fields such as cancer treatment. The most common NPs used in cancer treatment are $TiO_2$ NPs. Despite that the $TiO_2$ NPs are considered as harmless to people and animals; NPs are also considered as toxic. While the electrochemical and physical properties make these NPs proper to use in cancer treatment. Some of studies reported that $TiO_2$ NPs caused a massive toxicity to cancer cell line, while other studies consider the $TiO_2$ NPs as an alternative chemotherapeutic agent for cancer cell treatment, where the growth inhibition percentage increased with higher concentrations of NPs and longer exposure times.

The cytotoxicity mechanism of $TiO_2$ NPs is scientific interest to researchers. For instance, Lozano et al. reported that the cytotoxicity of $TiO_2$ NPs due to the presence of small aggregates formed by NPs can interact with the cell causing its death [25]. Also, some studies reported that $TiO_2$ NPs can migrate in the bloodstream by binding with plasma proteins, through the lymphatic system by macrophages, or to the bone marrow by monocytes [26]. The interactions between proteins and $TiO_2$ NPs are not well understood. Studies have showed that $TiO_2$ NPs have a net negative charge (at pH = 7), and bind to amino acids that containing –OH, –NH, and $–NH_2$ in their side chains [27].

In this study, the toxicity of $TiO_2$ NPs (extracted from toothpaste Sample D) of different concentrations (10, 20, 50, 100 and 200 µg/mL) was evaluated on four cell lines (Jurkat, HepG2, T-47D and S180) based on WST method. Figure 8 illustrates the results of four cell lines which were treated with varying concentrations of $TiO_2$ NPs extracted from toothpaste Sample D. In the Jurkat cell line, the presence of $TiO_2$ NPs (of different concentrations) did not cause cells death, but rather the percentage of the cells increased, which suggests that it had a positive effect on the growth of Jurkat cells. In T-47D and S180 cell lines, the percentage of cells increased in all concentrations of $TiO_2$ NPs, except at 100 mg/mL concentration, where the negative control experienced 0.476 % and 2.462 %, respectively, while the wells of 100 mg/mL $TiO_2$ NPs experienced 0.467 % and 2.432 % respectively (very little growth inhibition). But in the HepG2 cell line, the $TiO_2$ NPs (at all concentrations) caused a dramatic degree of toxicity.

**Table 7** The effect of $TiO_2$ NPs with different concentrations on the growth of different cell lines. The values are reported as mean of 3 replicates ± standard deviation.

| Sample | Cell growth inhibition (%) | | | |
|---|---|---|---|---|
| | Jurkat cell line | HepG2 cell line | T-47D cell line | S180 cell line |
| Positive Control | 0.459 ±0.089 | 2.318 ±0.107 | 0.397 ±0.039 | 2.243 ±0.148 |
| Negative Control | 0.560 ±0.024 | 2.345 ±0.007 | 0.476 ±0.028 | 2.462 ±0.127 |
| 10 mg/L $TiO_2$ NPs | 0.624 ±0.016 | 2.299 ±0.021 | 0.511 ±0.027 | 2.513 ±0.146 |
| 20 mg/L $TiO_2$ NPs | 0.565 ±0.021 | 2.341 ±0.006 | 0.475 ±0.011 | 2.487 ±0.122 |
| 50 mg/L $TiO_2$ NPs | 0.594 ±0.041 | 2.283 ±0.029 | 0.481 ±0.015 | 2.515 ±0.105 |
| 100 mg/L $TiO_2$ NPs | 0.688 ±0.050 | 2.331 ±0.029 | 0.467 ±0.017 | 2.432 ±0.128 |
| 200 mg/L $TiO_2$ NPs | 0.680 ±0.022 | 2.321 ±0.023 | 0.507 ±0.016 | 2.825 ±0.107 |

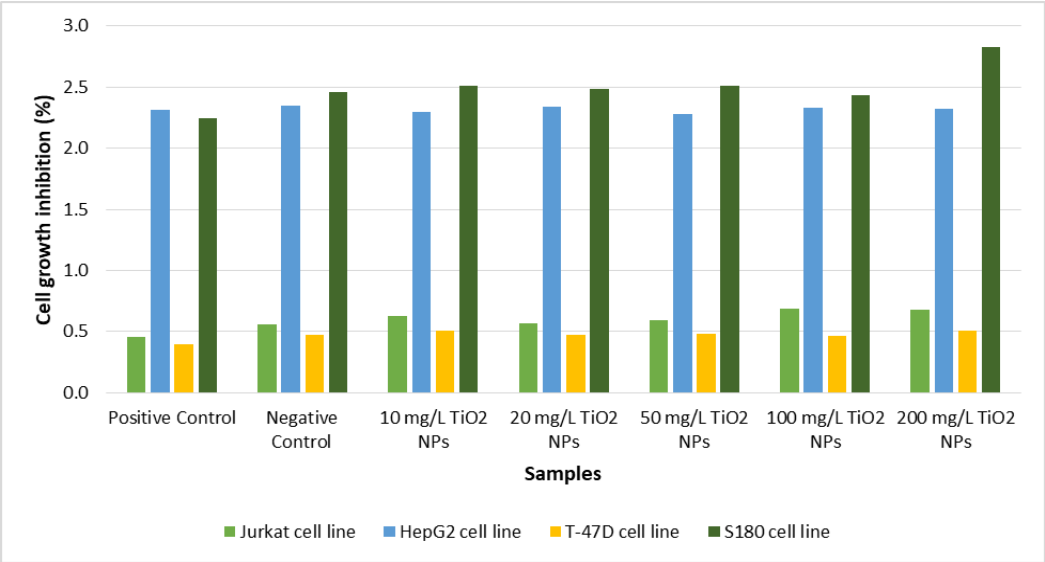


**Figure 8** The effect of $TiO_2$ NPs with different concentrations on growth of different cell lines.

The results showed that the $TiO_2$ NPs have a negative effect on the growth inhibition of the Jurkat,T-47D and S180 cancer cell lines, it may be due to short exposure time (48 h), and using low concentrations of the $TiO_2$ NPs, where these types of cancer (Leukemia, Breast cancer cell, and Sarcoma, respectively) are difficult to treat. $TiO_2$ NPs had a positive effect on the HepG2 cell line with the same exposure time and concentrations, liver carcinoma is considered as one of cancers that can easily be treated.

## 4. Conclusion

In summary, $TiO_2$ NPs have been extracted from toothpaste products by solid-liquid extraction method. The XRD results show that the mixture of $TiO_2$ NPs was formed (anatase and rutile titanium dioxide nanoparticles) with different sizes ranging from 2.5 to 53.2 nm. The toxicity effect of $TiO_2$ NPs was evaluated on *Chlorella Vulgaris* micro marine algae. The results indicate a negative effect on the growth algae and concentration of chlorophyll a during the early growth stages. In contrast, at the late growth stages these NPs have a positive effect. Also, the toxicity effect of $TiO_2$ NPs was evaluated on Jurkat, HepG2, T-47D and S180 cancer cell lines. The results showed that the $TiO_2$ NPs have a negative effect in the growth inhibition of the Jurkat, T-47D and S180 cancer cell lines. In contrary, a positive effect on the HepG2 cell line was observed. The results of this study confirm the importance of evaluating the environmental risks of nanoparticles by studying their interactions with different living systems.

## Compliance with ethical standards

*Acknowledgments*

We would like to thank Alia Mustafa and Fatima Hamad from Department of Physics, College of Science, Uni versity of Bahrain for their efforts and contribution in XRD and SEM analysis.

*Disclosure of conflict of interest*

The authors declared no conflict of interest.

## References

[1] Baca M, Wenelska K, Mijowska E, Kaleńczuk R J and Zielińska B. (2020). Physicochemical and photocatalytic characterization of mesoporous carbon/titanium dioxide spheres. Diam. Relat. Mater, 101, 1-10.

[2] Baranowska-Wójcik E, Szwajgier D, Oleszczuk P and Winiarska-Mieczan A. (2020). Effects of Titanium Dioxide Nanoparticles Exposure on Human Health—a Review. Biol. Trace. Elem. Res, 193(1), 118-129.

[3] Asadi A, Akbarzadeh R, Eslami A, Jen TC and Ozaveshe Oviroh P. (2019). Effect of synthesis method on NS-$TiO_2$ photocatalytic performance. Energy Procedia, 158, 4542-4547.

[4] Shi H, Magaye R, Castranova V and Zhao J. (2013). Titanium dioxide nanoparticles: a review of current toxicological data. Part. Fibre. Toxicol, 10(1), 1-33.

[5] Ziental D, et al. (2020). Titanium Dioxide Nanoparticles: Prospects and Applications in Medicine. Nanomaterials, 10(2), 1-33.

[6] Haghi M, Hekmatafshar M, Janipour MB and Seyyed S. (2012). Antibacterial effect of $TiO_2$ nanoparticles on pathogenic strain of E. coli. Int. J. Adv. Biotechnol. Res, 3(3), 621-624.

[7] Glass S, Trinklein B, Abel B and Schulze A. (2018). $TiO_2$ as Photosensitizer and Photoinitiator for Synthesis of Photoactive $TiO_2$-PEGDA Hydrogel without Organic Photoinitiator. Front. Chem, 6, 1-9.

[8] Behnam MA, Emami F, Sobhani Z and Dehghanian AR. (2018). The application of titanium dioxide ($TiO_2$) nanoparticles in the photo-thermal therapy of melanoma cancer model. Iran. J. Basic Med. Sci, 21(11), 1133-1139.

[9] Giusti A, et al. (2019). Nanomaterial grouping: Existing approaches and future recommendations. NanoImpact, 16, 1-18.

[10] Zhang Y, Leu Y R, Aitken R and Riediker M. (2015). Inventory of Engineered Nanoparticle-Containing Consumer Products Available in the Singapore Retail Market and Likelihood of Release into the Aquatic Environment. Int. J. Environ. Res. Public. Health, 12(8), 8717-8743.

[11] Ozkaleli M and Erdem A. (2018). Biotoxicity of $TiO_2$ Nanoparticles on Raphidocelis subcapitata Microalgae Exemplified by Membrane Deformation. Int. J. Environ. Res. Public. Heath, 15(3), 1-12.

[12] Thiagarajan V et al. (2019). Diminishing bioavailability and toxicity of P25 $TiO_2$ NPs during continuous exposure to marine algae Chlorella sp. Chemosphere, 233, 363-372.

[13] Hartmann N B, Von der Kammer F, Hofmann T, Baalousha M, Ottofuelling S and Baun A. (2010). Algal testing of titanium dioxide nanoparticles—Testing considerations, inhibitory effects and modification of cadmium bioavailability. Toxicology, 269, 190-197.

[14] Skjolding LM, Sørensen SN, Hartmann NB, Hjorth R, Hansen SF and Baun A. (2016). Aquatic Ecotoxicity Testing of Nanoparticles-The Quest to Disclose Nanoparticle Effects. Angew. Chem. Int. Ed, 55(49), 15224-15239.

[15] Jeffryes C, Gutu T, Jiao J and Rorrer GL. (2008). Metabolic Insertion of Nanostructured $TiO_2$ into the Patterned Biosilica of the Diatom Pinnularia sp. by a Two-Stage Bioreactor Cultivation Process. ACS Nano, 2(10), 2103-2112.

[16] Çeşmeli S and Biray Avci C. (2019). Application of titanium dioxide ($TiO_2$) nanoparticles in cancer therapies. J. Drug Target, 27(7), 762-766.

[17] Thevenot P, Cho J, Wavhal D, Timmons RB and Tang L. (2008). Surface chemistry influences cancer killing effect of $TiO_2$ nanoparticles. Nanomedicine Nanotechnol. Biol. Med, 4(3), 226-236.

[18] Joo KM, et al. (2019). Development and validation of UPLC method for WST-1 cell viability assay and its application to MCTT HCETM eye irritation test for colorful substances. Toxicol. *In Vitro*, 60, 412-419.

[19] Galletti A. (2016). Toxicity Evaluation of $TiO_2$ Nanoparticles Embedded in Consumer Products. Ph.D. thesis, University of Miami, USA.

[20] Ji J, Long Z and Lin D. (2011). Toxicity of oxide nanoparticles to the green algae Chlorella sp. Chem. Eng. J., 170(2-3), 525-530.

[21] Bakhshali-Dehkordi R, Ghasemzadeh MA and Safaei-Ghomi J. (2020). Green synthesis and immobilization of $TiO_2$ NPs using ILs-based on imidazole and investigation of its catalytic activity for the efficient synthesis of pyrimido[4,5-d]pyrimidines. J. Mol. Struct., 1206, 1-9.

[22] Gohari G, et al. (2020). Titanium dioxide nanoparticles ($TiO_2$ NPs) promote growth and ameliorate salinity stress effects on essential oil profile and biochemical attributes of Dracocephalum moldavica. Sci. Rep, 10(1), 1-14.

[23] Hund-Rinke K and Simon M. (2006). Ecotoxic Effect of Photocatalytic Active Nanoparticles ($TiO_2$) on Algae and Daphnids. Environ. Sci. Pollut. Res. Int., 13(4), 225-232.

[24] Mahmoodi NO, Ghavidast A and Amirmahani N. (2016). A comparative study on the nanoparticles for improved drug delivery systems. J. Photochem. Photobiol. B, 162, 681-693.

[25] Lozano T, et al. (2011). Cytotoxicity effects of metal oxide nanoparticles in human tumor cell lines. J. Phys. Conf. Ser, 304, 1-8.

[26] Olmedo D, Guglielmotti MB and Cabrini RML. (2002). An experimental study of the dissemination of Titanium and Zirconium in the body. J. Mat. Sci.: Materials in Medicine, 13, 793-796.

[27] Topoglidis E, Discher BM, Moser CC, Dutton PL and Durrant JR. (2003). Functionalizing Nanocrystalline Metal Oxide Electrodes with Robust Synthetic Redox Proteins. ChemBioChem, 4(12), 1332-1339.

[28] Tran TH, Nosaka AY and Nosaka Y. (2006). Adsorption and Photocatalytic Decomposition of Amino Acids in $TiO_2$ Photocatalytic Systems. J. Physical Chem, 110, 25525-25531.

## How to cite this article

Al-Salman F, Ali Redha A, Al-Shaikh H, Hazeem L and Taha S. (2020). Toxicity evaluation of $TiO_2$ nanoparticles embedded in toothpaste products. GSC Biological and Pharmaceutical Sciences, 12(1), 102-115.